Med Biol Eng Comput
DOI 10.1007/s11517-010-0594-1

ORIGINAL ARTICLE

Cardiogoniometric parameters for detection of coronary artery disease at rest as a function of stenosis localization and distribution

Thomas Huebner · W. M. Michael Schuepbach · Andrea Seeck · Ernst Sanz · Bernhard Meier · Andreas Voss · Roland Pilgram

Received: 11 October 2009 / Accepted: 28 February 2010

Abstract Cardiogoniometry (CGM), a spatiotemporal electrocardiologic 5-lead method with automated analysis, may be useful in primary healthcare for detecting coronary artery disease (CAD) at rest. Our aim was to systematically develop a stenosis-specific parameter set for global CAD detection. In 793 consecutively admitted patients with presumed non-acute CAD, CGM data were collected prior to elective coronary angiography and analyzed retrospectively. 658 patients fulfilled the inclusion criteria, 405 had CAD verified by coronary angiography; the 253 patients with normal coronary angiograms served as the non-CAD controls. Study patients—matched for age, BMI, and gender—were angiographically assigned to 8 stenosis-specific CAD categories or to the controls. One CGM parameter possessing significance ($P < .05$) and the best diagnostic accuracy was matched to one CAD category. The area under the ROC curve was .80 (global CAD versus controls). A set containing 8 stenosis-specific CGM parameters described variability of R vectors and R-T angles, spatial position and potential distribution of R/T vectors, and ST/T segment alterations. Our parameter set systematically combines CAD categories into an algorithm that detects CAD globally. Prospective validation in clinical studies is ongoing.

Keywords Cardiogoniometry · Vectorcardiography · R-T angle · CAD diagnosis · Depolarization–repolarization variability

1 Introduction

Coronary artery disease (CAD), myocardial ischemia, and acute myocardial infarction are among the most frequent causes of death in industrialized countries [26]. The presence of CAD is generally diagnosed according to angiographic criteria and defined as a reduction in coronary vessel lumen by at least 50%. Depending on the extent of plaque formation, concomitant inflammatory or repair processes (remodeling) along with atherothrombotic events (plaque rupture), CAD presents with multiple manifestations ranging from asymptomatic clinical pictures with silent myocardial ischemia to symptomatic, but stable CAD, across the spectrum of acute coronary syndromes (ACS) to sudden cardiac death (SCD). While interventional diagnostics (heart catheterization) is indicated in patients with verified signs of ischemia or manifest ACS, asymptomatic individuals with a high cardiovascular risk, atypical angina pectoris or stable to mildly symptomatic CAD, the indication for interventional diagnosis is best rendered by non-invasive methods such as stress electrocardiography (ECG), stress echocardiography, scintigraphy, and/or magnet resonance imaging. Clinically relevant coronary stenoses (>70%) can usually be treated by percutaneous coronary intervention or coronary artery bypass grafting.

T. Huebner (✉) · R. Pilgram
Department for Human and Economic Sciences, University for Health Sciences, Medical Informatics and Technology (UMIT), Eduard-Wallnoefer-Zentrum 1, 6060 Hall, Austria
e-mail: thomas.huebner@umit.at

W. M. Michael Schuepbach · E. Sanz · B. Meier
Department of Cardiology, University Hospital—Inselspital, Bern, Switzerland

W. M. Michael Schuepbach
Centre d'Investigation Clinique, CHU Pitié-Salpêtrière, Paris, France

A. Seeck · A. Voss
Department of Medical Engineering and Biotechnology, University of Applied Sciences Jena, Jena, Germany

Published online: 19 March 2010

Given that the disease and its precursors can take a long, asymptomatic course, typical complaints such as chest pain (angina pectoris) may be absent—even during an acute myocardial infarction [4]. With its many presentations, coronary atherosclerosis can be difficult to detect, especially in patients who cannot undergo stress testing. Thus, there is an unmet need for a practical, cost-effective method to improve diagnosis of CAD at rest in primary healthcare. In diagnosing CAD, standard 12-lead resting ECG can be inaccurate, particularly in stable and/or asymptomatic patients. Even in patients with ACS, the sensitivity of ECG for identifying non-ST-elevation myocardial infarctions and instable angina pectoris is low ($\sim$20%) [5]. In meta-analyses including patients without previous myocardial infarction, exercise ECG has shown a predictive accuracy of 69%, a sensitivity of 67%, and a specificity of 72% for CAD diagnosis [8]. However, exercise ECGs are often contraindicated medically or due to a negative effort-benefit ratio [8, 23]. Moreover, because of the effort and time required, exercise ECG is indicated only as a secondary assessment method in patients with a reasonable suspicion of CAD. Thus, ECG is not appropriate as a screening method for detecting CAD at rest in asymptomatic patients in primary healthcare.

As a simplified but improved alternative to ECG, cardiogoniometry (CGM) has been proposed for CAD detection [19, 20]. CGM is a spatiotemporal orthogonal-lead method using five electrodes and an automated diagnostic algorithm to analyze a 12-s vectorcardiographic recording in the resting patient. The method's simplicity and cost-effectiveness justifies its use in primary care settings.

Previously published CGM methods have achieved promising results in differentiating global CAD from non-CAD on retrospective cohorts [20–22]. However, when subsequently tested in prospective studies, some methods suffered from a markedly lower power to predict CAD [20]. In our analysis of this problem, we found that reason for this deviation between retrospective and prospective validity might have been that the localizations and distributions of coronary stenoses and ischemia patterns varied remarkably between the retrospective and prospective cohorts.

Likewise, other CGM algorithms have not systematically addressed parameters as a function of CAD category. Rather, they were optimized to the differentiation of global CAD versus non-CAD in a retrospective study population. The lack of a systematic approach and the partial non-suitability of certain parameters for certain CAD categories would potentially lead to a fall in the accuracy when applied to new study cohorts with different coronary stenosis localizations and distributions or ischemia patterns.

As a consequence, the authors developed the following hypotheses for examination in this study. First, the different CGM parameters are dependent on coronary stenosis localization and distribution. One CGM parameter is well suited for detecting a certain CAD category, but not necessarily suited for other CAD categories. Second, one significant parameter can be allocated to each one of the major CAD categories; this parameter will show the best possible sensitivity for detecting this CAD category with high specificity. The parameters found will be electrophysiologically plausible and consistent with the CAD or potential ischemia pattern.

Our primary aim was to deliver proof that at least one best-suited CGM parameter exists for each one of the 8 angiographically demonstrated stenosis-specific CAD categories that significantly differed from the non-CAD controls. Our secondary aim was to develop a parameter set that systematically covered all parameters found for the individual CAD categories, where every parameter can detect CAD in an equally ranked, parallel, and unweighted manner. In other words, this set of 8 parameters will form a universal algorithm that is independent of CAD category.

2 Materials and methods

2.1 Patients

A total of 793 patients with suspected non-acute CAD were analyzed. They constituted a cohort of patients who were consecutively admitted to the Department of Cardiology, Bern University Hospital over a 12-month period to undergo elective coronary angiography. Prior to coronary angiography, the study data were collected by resting 5-lead CGM on the supine patient using a proprietary CGM prototype [19, 20] equipped with software run at a 1000-Hz sampling rate and 16-bit resolution. During the recording, the patients were requested to hold their breath for 12–15 s after normal expiration. If this was not possible, they were asked to perform shallow breathing and keep their thoracic excursions to a minimum. The software automatically detected any ectopic and irregular beats occurring during the recording and excluded them from the analysis.

Exclusion criteria were atrial fibrillation, $\geq$50% ectopic beats during the recording, bundle branch blocks, severe (grade III) valvular heart disease, previous cardiac interventions, and previous myocardial infarction. A total of 135 patients were excluded. Of the 658 evaluable patients who were analyzed retrospectively, 405 had CAD verified by coronary angiography. The 253 patients with normal coronary angiograms served as the non-CAD controls. The patient characteristics are presented in Table 1.

CAD was defined using an empirical limit value of 50% for a stenosis in one or more of the three main coronary

Table 1 Patient characteristics including CAD categorization according to stenosis localization and distribution

Category	N (male)	Age	BMI	N (fem.)	Age	BMI	N (all)	Age	BMI
Controls	125	55.9 (11.7)	27.5 (10.8)	128	63.9 (10.1)	26.7 (5.4)	253	59.9 (11.6)	27.1 (6.5)
RCA	38	55.7 (10.7)	26.8 (10.8)	8	66.7 (6.8)	28.8 (5.2)	46	57.7 (10.9)	27.2 (10.3)
LAD	57	59.7 (11.5)	27.1 (3.4)	26	66.2 (11.5)	26.3 (4.1)	83	61.8 (11.8)	26.8 (3.6)
LCX	22	59.3 (10.8)	26.7(4.1)	4	70 (13.1)	29.9 (9.1)	26	60.9 (11.4)	27.2 (4.9)
RCA + LAD	27	62.3 (12.8)	28.6 (3.6)	14	71.2 (8.6)	25.8 (4.9)	41	65.4 (12.2)	27.7 (4.3)
RCA + LCX	20	58.4 (9.3)	26.7 (3.1)	5	64.0 (4.2)	32.3 (8.3)	25	59.5 (8.7)	27.8 (4.9)
LAD + LCX	40	66.9 (10.59)	26.2 (2.5)	15	69.3 (7.7)	26.5 (1.9)	55	67.5 (9.9)	26.3 (2.4)
RCA + LAD + LCX	103	67.3 (9.49)	27.6 (4.1)	26	70.4 (10.2)	22.9 (5.8)	129	68.0 (9.6)	26.5 (4.5)
CADall	307	62.7 (11.3)	27.2 (3.8)	98	68.6 (9.6)	27.5 (5.2)	405	64.9 (11.2)	27.3 (4.1)
Total	432	60.7 (11.8)	27.3 (6.6)	226	65.9 (10.2)	27.2 (5.3)	658	62.5 (11.6)	27.3 (6.2)

Number (N), age, and body mass index (BMI) of non-CAD controls and CAD patients in the different CAD categories stated as mean (standard deviation). As shown, the categories are comparable for age and BMI

arteries RCA (right coronary artery), LAD (left anterior descending artery), and LCX (left circumflex artery).

This study was approved by the local ethics committee, and all patients gave their written informed consent.

2.2 Principles of cardiogoniometry

The trigonometric principles of CGM as illustrated in Fig. 1 have been published in detail elsewhere [19, 20]. Four electrodes define two planes perpendicular to each other. Vectorial addition of the potentials measured between three electrodes in each plane yields a vector that corresponds to the projection of the heart vector into this plane. Using the vector projections in the two orthogonal planes, the heart vector can be reconstructed for every millisecond. Vector orientation indicates the direction and vector length the strength of the electrical field generated by the heart.

Three mutually orthogonal projections X, Y, and Z are trigonometrically calculated out of three bipolar derivatives, A, D, and Ve (Figs. 1b and 2). The use of a Cartesian coordinate system (XYZ) orientated roughly according to the anatomy of the heart and its orientation in the chest is greatly advantageous for visualization of spatial de- and repolarization and to provide an immediate cardiologic understanding of the recorded vectorial information. The X-axis has an anteroposterior orientation (values with positive signs have a posterior location). The Y-axis has a left-oblique-sagittal baso-apical orientation (values with positive signs point to the apex and those with negative signs to the base of the heart). The main plane (oblique sagittal plane) is defined by the X- and Y-axes. The Z-axis is perpendicular to the two other planes (values with negative signs point up). The frontal plane is defined by the Y- and Z-axes. The plane defined by the X- and Z-axes is also a sagittal plane, which is perpendicular to the oblique sagittal and frontal planes and separates the apical and basal portions of the heart.

For better quantification of the spatial information of the CGM vector-loops, the space can be divided into eight octants by the three planes. Parts of the loops within each octant can be quantified (Figs. 1b and 2a, b). The projections of every vector and, above all, the maximum vectors of each loop projected onto an imaginary sphere around the heart and with the coordinate origin (intersection of the X-, Y-, and Z-axes) at the centre can be defined by the longitudinal and latitudinal coordinates on a globe (Fig. 2a, b).

The angle alpha defines the degree of longitude (the meridian), i.e., how far the vector is in front of or behind the YZ plane. The angle alpha of a vector lying in the Y-axis and pointing toward the apex is defined as 90°. Points on the apical hemisphere have a positive angle alpha (0° to 180°); points on the basal hemisphere have a negative angle alpha (0° to −180°). The angle beta defines the degree of latitude, i.e., the value by which a vector lies above or below the XY plane (oblique sagittal or main plane). Positive values of the angle beta indicate that the vector points to below the oblique sagittal plane, whereas negative values are assigned to angles above the oblique sagittal plane.

A planar illustration of spatial cardiogoniometry was generated from the XZ projection with a view onto the apex of the heart by folding up the basal parts of the heart. This is comparable to a spherical, elliptical, and planar map created by flattening out a globe (Fig. 2a).

CGM differs from conventional 7-lead Frank vectorcardiography in two essential respects. First, CGM is recorded with 5 leads (4 electrodes and one ground) without intercalated resistor networks (uncorrected technique). The geometrical electrode placement in an orthogonal system avoids the distortions associated with vectorcardiography techniques [19]. In CGM, the electrode

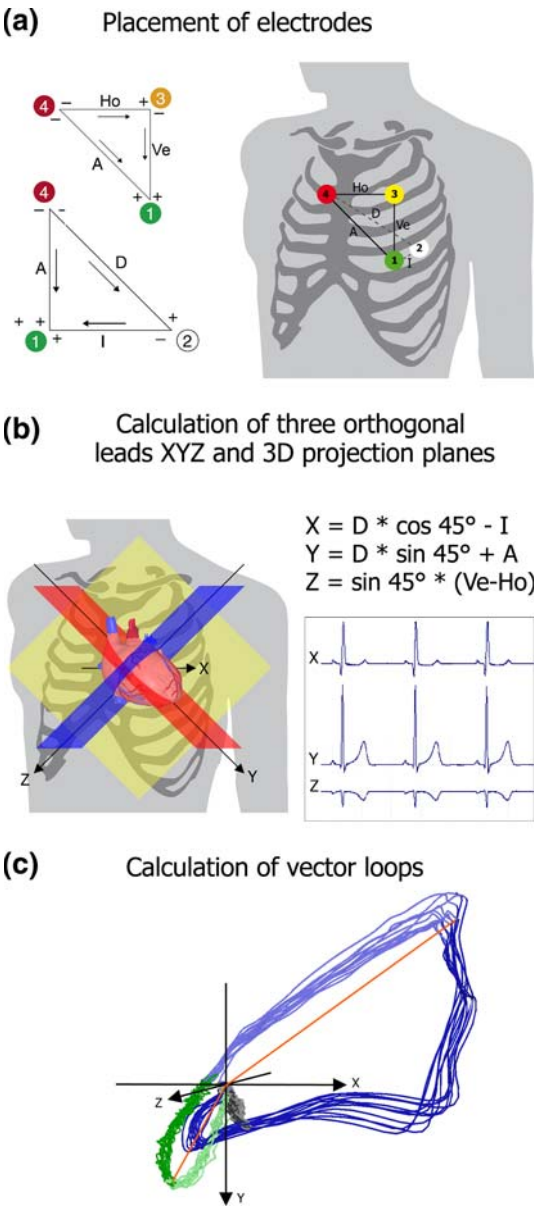

◀**Fig. 1** Principles of cardiogoniometry. **a** The four signal electrodes are placed on the thorax: at point 1 (*green*), equivalent to point V4 of Wilson, in the 5th intercostal space in the midclavicular line; at point 2 (*white*) sagittal to electrode 1 on the back (point V8 of Wilson); at point 3 (*yellow*) perpendicularly above electrode 1 at 0.7 times the distance between points 1 and 2; at point 4 (*red*) to the right of point 3 at the same distance as between points 1 and 3. The fifth electrode is ground and can be attached somewhere above the right hip. The leads are defined as: 4-2 D (*dorsal*), 4-1 A (*anterior*), 2-1 I (*inferior*), 4-3 Ho (*horizontal*), 3-1 Ve (*vertical*). **b** Points 4-2-1 define the oblique sagittal plane (OSP) (*red*); points 4-3-1, the frontal plane (*yellow*). The third plane (*blue*) is orthogonal to the two other planes and contains point 3; it is the sagittal plane perpendicular to the OSP. Projection x is orientated in an anterodorsal direction and lies in the OSP and the sagittal plane perpendicular to the OSP. Projection Y is orientated in a baso-apical direction and lies in the OSP (4-2-1) and the frontal plane (4-3-1). Projection Z is orientated in a supero-inferior direction relative to the OSP and lies in the frontal plane (4-3-1) and the sagittal plane perpendicular to the OSP (19). **c** Vector-loops can be calculated within a Cartesian coordinate system using X, Y and Z coordinates of the heart vector at each ms recording. Note the R-loops (*blue*) and T-loops (*green*) of 12 heart cycles and maximum vectors of both loops (*red*). The maximum vectors are calculated on the median loops

position and the trigonometrical constructions lead to a mathematically correct orthogonality of XYZ projections. Secondly, CGM projection planes are not aligned with the body planes but rotated to approximately match the anatomical orientation of the heart similar to the short axis scan of an MRI.

A total of 350 parameters can be extracted from the CGM data fully automatically and divided into main classes: Angles consisted of the angles alpha and angle beta of the P-, R-, and T-loops, in particular, the angle of the maximum vectors and at further defined positions in the loops and angles between the maximum vectors of the P-, R-, and T-loops. The amplitude class comprised the minima/maxima and amplitude ratios of P, R, and ST/T segments. Shapes and eccentricities were used to describe the P-, R-, and T-loops. Potential distributions covered the P-, R-, and ST/T-loops in the octants 1-8. Velocities were classified as absolute values and ratios of the P-, R-, and T-loops. Additionally, all parameters were classified according to variability.

2.3 Statistical analysis

All calculations and statistical analyses were performed using MATLAB (The MathWorks, Inc., Natick, MA, USA). The unpaired two-sided non-parametric Mann–Whitney U test was used to test for significance. The correlation analyses were performed using Kendall's tau rank correlation coefficient (τ).

To describe and compare the accuracy of our overall parameter set, we plotted its total sensitivity versus its total specificity (global CAD versus non-CAD controls) on a multivariate receiver operating characteristic (ROC) curve according to Step (E) below.

2.4 Parameter derivation and set compilation

Based on our hypotheses, we systematically derived our CGM parameters and compiled them into an overall set using the steps detailed below (A–E): The aim was to identify 8 parallel and equally ranked parameters for global CAD detection. In other words, the parameter set can only classify a patient as healthy when all 8 parameters are located within the range predefined as normal. Whenever a single parameter falls outside the normal range, the patient is defined as CAD positive.

(A) First, we subdivided CAD categories according to stenosis localization and distribution as determined in the

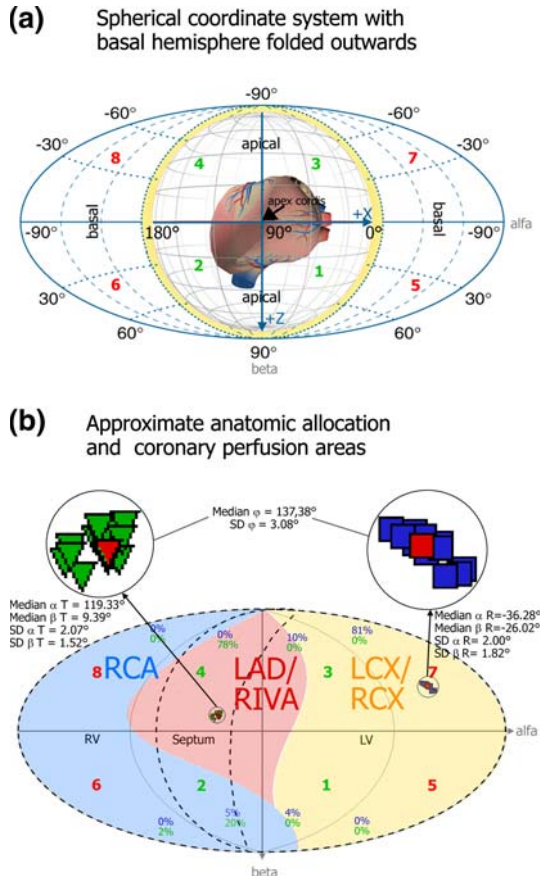

Fig. 2 Spherical coordinate system, octants apportionment, and perfusion map. **a** The coordinate system of the three orthogonal axes and the three planes divide the imaginary sphere into eight octants roughly relating to the heart's anatomy (see also Fig. 1b). Octants 1–4 are apical (*green numbers*), 5–8 are basal (*red numbers*). Octants 1, 2, 5, 6 represent the posterior wall (inferior in relation to the heart), and octants 3, 4, 7, and 8, the anterior wall (superior in relation to the heart). Octants 1, 3, 5, 7 represent the left ventricle (posterior in relation to the heart), and octants 2, 4, 6, and 8 map the septum and right ventricle (anterior in relation to the heart). **b** In normal coronary predominance, the RCA perfuses octants 8, 6, and, partially, 2. The LAD predominately perfuses octant 4 and, partially, 2 and 3; the LCX mainly perfuses the left ventricular octants 1, 3, 5, and 7. The maximum vectors of the R-loops (*blue rectangles*) and T-loops (*green triangles*) of 12 sequential cycles of a patient example are presented. The circles around the cluster represent the variability or standard deviation of the maximum vectors. In the upper and lower part of the ellipse, the potential distributions of the R-loops (*blue*) and T-loops (*green*) at the 8 octants are indicated in percent (the sum of all loops always equals 100%)

elective coronary angiography. The AHA model of 15 coronary segments [1] was not applicable for categorization because it would have created too many categories of too few patients each. Instead, we restricted our CAD categorization to three main coronary arteries and their combinations (see Table 1): 3 categories with single-vessel stenoses (RCA, LAD, LCX), 3 categories with two-vessel stenoses (RCA + LAD, RCA + LCX, LAD + LCX—including left main coronary artery stenoses), 1 category with three-vessel stenoses (RCA + LAD + LCX), and the global CAD category.

(B) Parameters that differed significantly ($P < .05$) between patients in a specific CAD category compared to non-CAD controls were considered in the further analysis (C) for that specific CAD category.

(C) Every single CAD category was compared with the non-CAD category by determining the area under the receiver operator characteristics (ROC) curve (AUC) for each of the significant parameters at a single specificity downward between 100 and 90% (AUC100-90). For this purpose, the single specificity was lowered in 0.1% decrements between 100 and 90% for each parameter; the respective sensitivities (individually for each CAD category) and cut-off values were also recorded. The parameter at maximum AUC100-90 was regarded as the most suitable per CAD category. AUC100-90 were produced for the two genders and summarized in one value, although different cut-off values were possible for women and men.

(D) Eight parameters were obtained by this method (AUC100-90max), one per CAD category. To test their mutual independence, all 8 parameters were cross-correlated with each other. Whenever two parameters correlated too strongly (criterion $\tau > 0.6$), the one with the lower AUC100-90 in its CAD category was excluded. The next most suitable parameter was moved up to replace the excluded parameter before all 8 parameters were combined into a set for diagnosing global CAD. This set now consisted of 8 parameters, each of which was proven significant and mutually independent, and possessed the largest average sensitivity for its respective CAD category in the single specificity range of 100–90%.

(E) For all CAD patients versus controls, we lowered in equal and parallel measure the single specificity for each parameter in decrements of 0.1% starting from 100%. Then, we used the total specificity and total sensitivity obtained in each step to plot the multivariate ROC curve for the overall parameter set.

3 Results

3.1 Parameters

Table 2 presents the significance of parameters in CAD categories compared to non-CAD controls. The underlined *P* values indicate the significant parameter for each CAD category that met the criterion AUC100-90max and was regarded as the most suitable and stable for identifying that CAD category. The 8 parameters, including their units of measure in square brackets, are explained as follows:

P51 "SD betaRmax" [°]: This parameter indicates the standard deviation (variability) of angle beta of the XYZ

Table 2 Significance of parameters in CAD categories compared to non-CAD controls (*P* values)

Parameters	RCA	LAD	LCX	RCA + LAD	RCA + LCX	LAD + LCX	RCA + LAD + LCX	CADall
P051	ns	ns	<.05	ns	ns	<u><.05</u>	≪.001	≪.001
P064	<.001	≪.001	<.01	ns	<u>≪.001</u>	ns	ns	ns
P072	ns	<.01	<.05	<.05	<.05	<.05	<u>≪.001</u>	≪.001
P155	ns	<u><.01</u>	ns	<.01	ns	<.01	ns	<.05
P285	<u><.001</u>	ns	<.05	ns	ns	ns	ns	ns
P301	<.001	ns	<u>≪.001</u>	<.05	<.05	ns	≪.001	≪.001
P304	ns	≪.001	ns	≪.001	ns	<.01	≪.001	<u>≪.001</u>
P306	ns	<.01	<.05	<u><.01</u>	ns	≪.001	≪.001	≪.001

The underlined *P* values represent the most suitable parameters for the respective CAD category, selected by maximum AUC100-90 and significance ($P < 0.05$) using the unpaired two-sided non-parametric Mann–Whitney U test

ns not significant

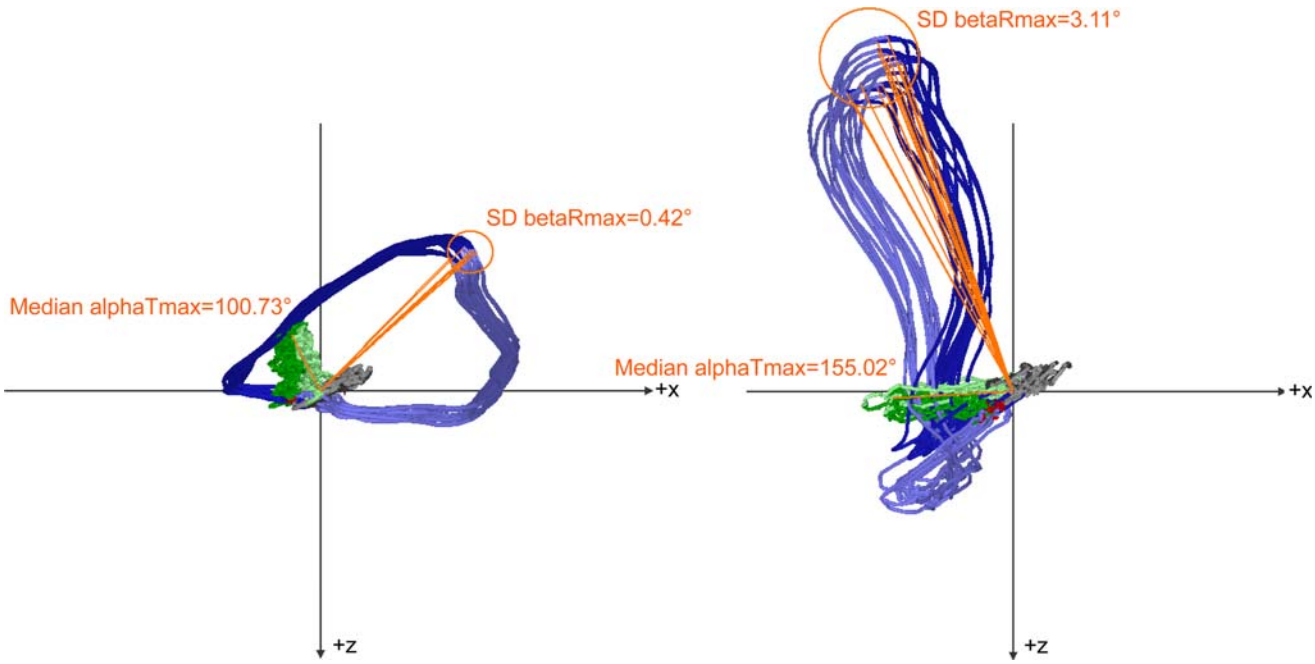

Fig. 3 Parameters P64 "Median alphaTmax" and P51 "SD betaRmax." The graphic shows the CGMs of a non-CAD (*left*) and a CAD patient (*right*). The P-loops (atrial excitation, *gray*), R-loops (depolarization phase, *blue*), and T-loops (repolarization phase, *green*) of a 12-s recording are depicted. Red indicates the maximum vector of all R-loops and the T-loop of the median complex. Parameter 64 "Median alphaTmax" shows the angle alpha (on the X-axis) of the maximum vector of the T-loop. Parameter P51 "SD betaRmax" represents the standard deviation (variability) of the maximum vectors of all R-loops on the recording

vectors at time point Rmax (on the Z-axis in the XZ projection). Rmax is the point at which the summation vector in the depolarization phase is the largest (Fig. 3). In general, this parameter defines heterogeneities in the depolarization phase, and, in particular, fluctuations in the axis between anterior and posterior wall.

P64 "Median alphaTmax" [°]: This parameter is defined as angle alpha of the XYZ vector at time point Tmax (on the X-axis in the XZ projection), measured at the T-loop of the median cycle. Tmax is the point at which the summation vector in the repolarization phase is the largest (Fig. 3). A shift in this parameter, particularly into the region of the right ventricle/septum (the angle alpha of Tmax increases to above 90°) may indicate a more ischemic lateral left ventricle (compared to the right ventricle) or possibly a hypertrophic septum.

P72 "SD phi" [°]: This parameter indicates the standard deviation (variability) of angle "phi," defined as the opening angle between the vectors in Rmax and Tmax, i.e., the spatial opening angle between maximum de- and repolarization (equal to R-T or QRS-T angle). In general, this parameter indicates heterogeneities and fluctuations between the de- and repolarization phase between the individual cycles.

P155 "Mean TOct5" [%]: This parameter indicates the percentage of the STT-loop potential (from J-point to T-end) that lies in the octant 5. The sum of all 8 octants always adds up to 100%. This parameter was calculated using the STT-loop average. Normally, there is almost no T-potential in octant 5. As the STT potential moves away from a region that is ischemic, an increase of T-potential in octant 5, representing the basal left ventricular region of the posterior wall, may indicate contralateral ischemia. An elevation in the STT potential distribution in octant 5 suggests an ischemic change in the spatially contralateral octant 4 (apical right ventricular portion of the anterior wall and anterior portions of the septum), where octant 4 is normally mainly perfused by the LAD (see Fig. 2b).

P285 "alpha R + Dir" [°]: This parameter describes the spatial direction of the R-loop halfway between the beginning of the Q wave and Rmax, calculated from the R-loop of the median cycle. The spatial tangent was placed by computing the differential vector 4 ms in front of and behind point R/2 and by measuring the angle alpha of this vector in relation to the X-axis of the XZ projection. At an angle alpha of 90°, the tangent would be exactly perpendicular to the X-axis which would indicate an electrical equilibrium between the right ventricle including septum (RV/S) and the left ventricle (LV) in the ascending depolarization phase. At a value of ≥90°, the tangent of the ascending R-loop points away from RV/S and in the direction of the LV. This may indicate a more ischemic RV/S (compared to the LV) and/or left ventricular hypertrophy (LVH).

P301 "MinX T" [mV]: This parameter is defined as the minimum voltage occurring in all cycles measured in the STT segment between J-point and T-end in projection X, mostly at the J-point or Tmax at a negative T. The orientation of projection X is sagittal to the frontal plane of the body when viewed from the anterior (negative voltages) to the posterior (positive voltages). Projection X depicts the voltage curve from the right to the left ventricle. A too low value of minimum X in the STT segment thus corresponds to a shift from x in the direction of the right ventricle and indicates left ventricular ischemia.

P304 "MaxY T" [mV]: This parameter is defined as the maximum voltage occurring in all cycles measured in the STT segment between J-point and T-end in projection Y. It is mostly located at Tmax. Projection Y basically represents the voltage curve within the oblique sagittal plane on the basal–apical axis. In the normal state, positive voltages point to the apex of the heart. Therefore, a too small maximum value of MaxY T suggests ischemia in the apical regions.

P306 "MaxZ T" [mV]: This parameter is defined as the maximum voltage occurring in all cycles measured in the STT segment between J-point and T-end in projection Z, mostly Tmax. Basically, projection Z represents the voltage curve from the left axillary (negative voltages) to the sternal xiphoid process (positive voltages) running perpendicular to the oblique sagittal plane. Thus, this axis tends to point from the anterior (negative voltages) to the posterior wall (positive voltages). A too large value of maximum Z of T indicates anterior wall ischemia.

3.2 Accuracy of the parameter set

We tested the accuracy of the parameter set on all CAD patients compared to non-CAD controls. The multivariate ROC curve derived according to Step E is shown in Fig. 4. The AUC was .80. For example, a local optimum on the ROC curve was located where an overall specificity of 76.3% (95% confidence interval: 70.6–81.4%) intersected an overall sensitivity of 72.1% (95% confidence interval: 67.5–76.4%). Here, the specificity of each single parameter is 95.3%.

Table 3 lists the sensitivities of the 8 parameters for the CAD categories at this exemplary specificity of 95.3%, similarly the respective sensitivity, specificity, positive (PPV), and negative predictive value (NPV) of the overall parameter set. The underlined numbers indicate the significant parameter determined to best describe one CAD category ($P < .05$), where the criterion AUC100-90max was met and which was regarded as the most suitable and most stable for that CAD category.

All CAD categories and the controls were relatively matched for age and body mass index (BMI) (Table 1). Men and women were analyzed separately in the algorithm in that all parameters for both genders were allocated separate cut-off values. To exclude any other dependency on age and BMI, all parameters in the non-CAD controls, the CADall category, and the overall cohort were correlated with age and BMI (each subdivided into male only, female only, and both genders) (Table 4). Since only a fractional correlation to age and BMI, calculated as the mean absolute value for all parameters ($\tau = 0.07 \pm 0.05$), was found, it could be ruled out that these variables had any major influence on the patient cohort.

4 Discussion

With the overriding aim to establish a practical, cost-effective method to improve electrocardiological diagnosis of coronary artery disease (CAD) at rest in primary healthcare, this retrospective study systematically tested a series of parameters using a cardiogoniometric setup on a cohort of 793 patients with presumed non-acute CAD.

Since the late 1930s, alternatives to ECG like vectorcardiography (VCG) and various different lead-placing methods have been proposed [25] and developed [2]. The best-known and most frequently used VCG method is the 7-lead method developed by Frank [7]. VCG—a popular and widely published method of the past decades—was

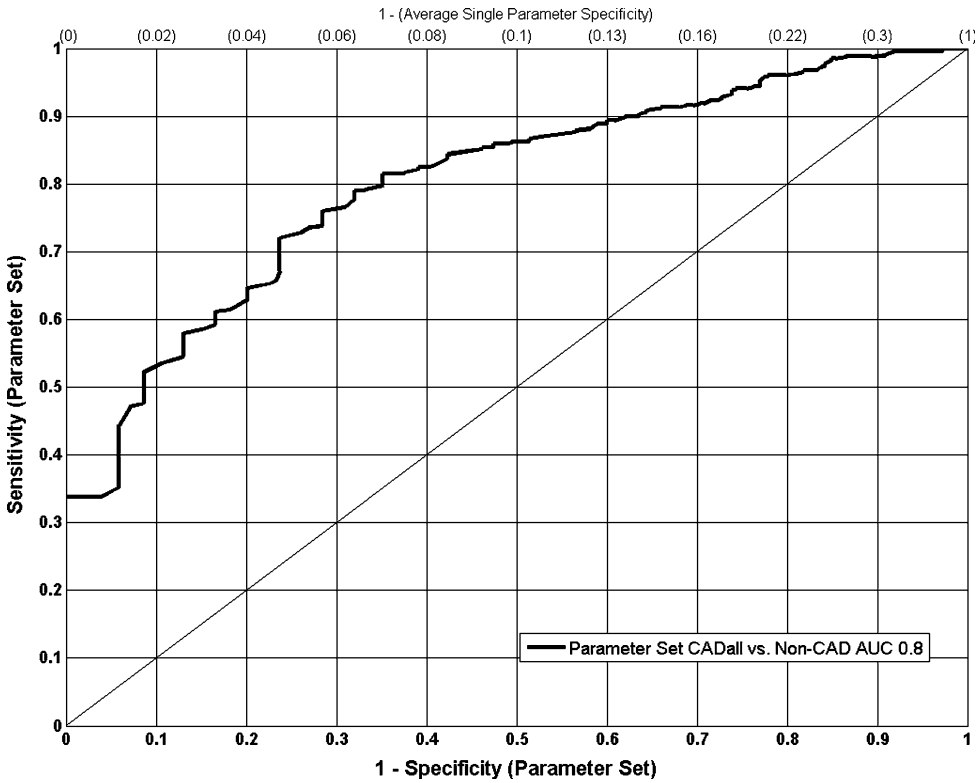

Fig. 4 Multivariate ROC curve of the parameter set distinguishing all CAD patients from non-CAD controls. The upper X-axis shows the average single parameter specificity; the lower X-axis shows the total specificity with the respective sensitivity (Y-axis)

Table 3 Sensitivity of CGM parameters in CAD categories plus CADall versus non-CAD controls chosen at the local optimum of the overall ROC curve and leading to a single specificity of 95.3% per parameter (top). Similarly the respective sensitivity, specificity, positive (PPV), and negative predictive value (NPV) of the overall parameter set (bottom)

Parameters	RCA (%)	LAD (%)	LCX (%)	RCA + LAD (%)	RCA + LCX (%)	LAD + LCX (%)	RCA + LAD + LCX (%)	CADall (%)
P051	(6.5)	(15.7)	11.5	(17.1)	(20.0)	20.0	23.3	17.8
P064	15.2	4.8	26.9	(17.1)	20.0	(12.7)	(20.2)	(15.6)
P072	(13.0)	19.3	15.4	14.6	24.0	14.5	31.0	21.2
P155	(10.9)	26.5	(19.2)	26.8	(28.0)	27.3	(16.3)	21.2
P285	26.1	(8.4)	23.1	(2.4)	(12.0)	(16.4)	(9.3)	(12.3)
P301	15.2	(6.0)	42.3	12.2	8.0	(12.7)	16.3	14.3
P304	(13.0)	27.7	(23.1)	31.7	(20.0)	25.5	29.5	25.9
P306	(10.9)	21.7	19.2	24.4	(8.0)	30.9	25.6	22.2
Sensitivity	63.0	65.1	76.9	73.2	76.0	80.0	74.4	72.1
Specificity	76.3	76.3	76.3	76.3	76.3	76.3	76.3	76.3
Prevalence	7.0	12.6	4.0	6.2	3.8	8.4	19.6	61.6
PPV	16.7	28.4	11.8	17.0	11.2	23.5	43.4	83.0
NPV	96.5	93.8	98.8	97.7	98.8	97.7	92.4	63.1

The underlined sensitivities represent the most suitable parameters for the respective CAD category

( ) not significant

mainly used to diagnose ischemia, CAD, and myocardial infarction at rest [6, 9–11, 13–15, 24]. Although VCG is accepted and proven in principle, it never became widely established in general clinical use because it was too complicated to record and difficult to interpret, later to be overtaken by coronary angiography and nuclear-medical imaging methods. Nowadays, vectorcardiographic analysis is mainly used to analyze the spatial and temporal heterogeneity of the repolarization phase (i.e., T-wave variability and T-wave alternans), and for risk stratification ranging from ventricular tachyarrhythmia (VT) to sudden cardiac death (SCD) [3, 17, 18].

Table 4 Correlation of all parameters with age and body mass index (BMI) in non-CAD controls, the CADall category, and overall cohort (subdivided into male only, female only and both genders) is presented as the mean absolute value of Kendall's tau rank correlation coefficient (|τ|)

Parameters	Non-CAD controls			CADall			Overall cohort CADall + controls		
	(Male)	(Fem.)	(All)	(Male)	(Fem.)	(All)	(Male)	(Fem.)	(All)
P051—Age	0.10	0.04	0.14	0.08	0.12	0.11	0.13	0.10	0.10
P051—BMI	0.16	0.14	0.14	0.15	0.16	0.14	0.17	0.15	0.15
P064—Age	0.06	0.13	0.02	0.00	0.05	0.05	0.02	0.01	0.01
P064—BMI	0.06	0.03	0.01	0.00	0.09	0.03	0.01	0.06	0.06
P072—Age	0.02	0.05	0.04	0.05	0.08	0.04	0.09	0.08	0.08
P072—BMI	0.07	0.00	0.03	0.10	0.09	0.10	0.11	0.04	0.04
P155—Age	0.07	0.07	0.09	0.11	0.11	0.06	0.11	0.00	0.00
P155—BMI	0.03	0.12	0.07	0.11	0.24	0.14	0.08	0.17	0.17
P285—Age	0.08	0.06	0.02	0.06	0.02	0.02	0.06	0.00	0.00
P285—BMI	0.14	0.05	0.09	0.06	0.11	0.06	0.08	0.08	0.08
P301—Age	0.04	0.10	0.04	0.02	0.15	0.00	0.00	0.15	0.15
P301—BMI	0.13	0.11	0.11	0.05	0.16	0.01	0.06	0.02	0.02
P304—Age	0.01	0.17	0.02	0.06	0.04	0.09	0.09	0.01	0.01
P304—BMI	0.10	0.00	0.03	0.05	0.03	0.03	0.08	0.01	0.01
P306—Age	0.02	0.07	0.11	0.11	0.18	0.15	0.12	0.15	0.15
P306—BMI	0.07	0.03	0.01	0.04	0.06	0.01	0.06	0.03	0.03

As an advancement of the vectorcardiographic principle, a cardiogoniometric method using a score for identification of CAD has been prospectively validated on 332 patients against coronary angiography findings (stenosis >50%) showing an overall diagnostic sensitivity of 64% and a specificity of 82% [20]. Other attempts to develop CGM methods for CAD detection retrospectively tested the suitability of multivariate analysis methods in smaller and dedicated cohorts, using methods such as logistic regression (345 patients, sensitivity 66%, specificity 77%) [21], linear discriminant analysis (109 female patients, sensitivity 81%, specificity 90%), and support vector machines (109 female patients, sensitivity 79%, specificity 87%) [22]. These methods mostly combined additive and weighted parameters into one function; their approach was less systematic and CAD categories were not formed. When subjected to prospective validation, these methods showed instability in cohorts with differing stenosis distribution patterns.

With an overall sensitivity of 72.1% and specificity of 76.3%, the accuracy of the method presented here was, in part, lower than previously published retrospective multivariate analyses. Nevertheless, the results of this study were obtained on a larger and non-selected all-comer cohort of 793 patients. Likewise, the main emphasis was not on a retrospectively optimized result, but rather on proving that the systematic approach would prospectively show better stability in diagnosing CAD independently of coronary-stenosis type and distribution.

Given that CAD stenoses occur in a variety of distributions and combinations, it was the authors' hypothesis that the different CGM parameters, e.g., representing spatial angles and potential distributions in the de- and repolarization phases, are altered during pathological states and that this alteration depends on the localization and size of the myocardial region affected by CAD. Thus, we assumed that pathological CGM findings represent disequilibria and heterogeneities in the electrical activity of the myocardium. Because it affects a circumscribed myocardial region, a flow-limiting single-vessel stenosis could result in a shift of the summation vector of total electrical myocardial activity away from the diseased region. A two- or three-vessel stenosis would potentially consist of two or more spatially contralateral stenoses; this effect may be compensated by changes that tend to displace the summation vector in opposite directions and thus produce a "stalemate" situation with the vector remaining in a normal position. Therefore, particular CGM parameters would be sensitive and specific for the different possible changes in the distribution of myocardial perfusion resulting from different coronary artery alterations.

Thus, and because CGM parameters are not equally valid for all CAD categories, the present method developed a CGM parameter set using unweighted, parallel and equally ranked parameters to detect CAD independently of cohort composition.

Herein, we proved our hypothesis that the different CGM parameters are dependent on coronary stenosis

localization and distribution. Thereby, we established the existence of one CGM parameter that was most suited for detecting one of the 8 angiographically demonstrated stenosis-specific CAD categories versus non-CAD controls. While we were able to assign at least one CGM parameter to one CAD category with statistical significance compared to non-CAD controls, no one parameter significantly defined all CAD categories. This would explain why not every CGM parameter was suitable for all CAD categories in the same way. Also, we were able to allocate to each CAD category one parameter that showed the best possible sensitivity for detecting that category with high specificity.

Further, the parameters we found appeared to be electrophysiologically plausible and consistent with CAD or potential ischemia patterns. We used these 8 parameters as discriminating indices to develop a set that systematically covered all parameters found for the individual CAD categories, where each parameter was able to detect CAD in an equally ranked, parallel and unweighted manner.

The parameters presented in the Results section serve as experimental models to explain how the parameters were made plausibly consistent with CAD or ischemia patterns. Specifically, the cardiogoniometric parameters MinX T, MaxY T, und MaxZ T (P301, P304, P306) most closely approximated ST-segment depressions and T-inversions on the ECG [5, 8], albeit using bipolar orthogonal leads. Two of our parameters describe spatiotemporal variabilities: SD betaRmax (P051), the standard deviation of the Rmax vector within the depolarization phase; and SD Phi (P072), the standard deviation of the R-T angle reflecting the interaction between the de- and repolarization phases. Compared to most publications that considered alternans phenomena, variabilities and heterogeneities in the repolarization phases for risk stratification [3, 17, 18, 27], our approach is essentially new in that we included the variability effects of the depolarization phase for detecting CAD. The parameters median alphaTmax (P064) and median TOct5 (P155) describe spatial positions and potential distributions of the repolarization phase, while the parameter alpha R + Dir (P285) indicates a spatial position in the depolarization phase. Earlier vectorcardiographic methods similarly used parameters for describing spatial positions of various segments of the vector-loops [2, 6, 7, 9, 11, 13–15, 24].

We may have improved on a previous publication that compiled a total of 18 CGM parameters into 2 gender-dependent scores, but did not systematically categorize or equally rank the distributions and combinations of coronary stenoses as we have done [20]. Dependency on the differing compositions of the retrospective and prospective cohorts is the likely reason that the sensitivity and specificity obtained in another retrospective analysis dropped in the prospective analysis by 9 and 5%, respectively [20]. Our algorithm is designed to be inherently independent of study sample composition. That way, the effect of coronary stenosis localization, distribution, and ischemia pattern on the power of the parameter set should also be minimized when tested on future cohorts.

4.1 Study limitations

One limitation of the CGM method presented in our study was that it assigned coronary stenoses to parameters that describe electrical myocardial activity locally without taking into account the type of coronary predominance. Also, because some category sizes were small, further cross validation and stratification according to coronary predominance were not performed and will have to be addressed by future studies. The influence of ventricular hypertrophy should similarly be explored in greater detail. Also, patients who have bundle branch blocks, atrial fibrillation and previous MI, i.e., the exclusion criteria in our study, should be investigated.

The overall parameter set achieved an acceptable AUC of .80 and a sensitivity of 72.1% at a single specificity of 95.3% per parameter in all CAD patients versus non-CAD controls. However, the set's overall specificity of 76.3% at this arbitrary cut-off point may limit its suitability for screening. One reason for this may be that the control group did not consist of truly "healthy" individuals, but of patients with suspected non-acute CAD in whom elective coronary angiography only ruled out significant coronary stenoses >50%.

4.2 Generalizability of our parameter-set approach to decision-making algorithms

Additionally, we explored whether our method of creating a parameter set for decision-making algorithms might be generalizable to other indications. Our method is capable of analyzing a variety of biosignals and is particularly suited as a decision-making algorithm for detecting clinical pictures comprising different disease categories or of several individual diseases with different (spatial) manifestations. This advantage would particularly apply whenever such individual categories are defined by intrinsic or independent parameters and/or patient cohorts have to be investigated where cohort composition may be subject to great inter-category variability. For example, in one study, 12 different electromyographic and acceleration signal features were extracted and subjected to principal component analysis (PCA) to detect Parkinson's patients [16]. Because different symptoms prevail during various stages of Parkinsonism, our approach of parameter finding and set compilation might be used as an alternative to PCA for decision making in this context.

Another application for our algorithm might be to detect depression based on electroencephalographic indicators similar to a study that compared the sensitivity of different electroencephalographic indicators and parameters like spectral asymmetry index, inter-hemispheric asymmetry, and coherence methods for the detection of depression [10]. Our set compilation approach could be particularly useful for combining indicators and extended parameters to analyze cortically and spatiotemporally variable parameters.

4.3 Choice of reference standards for CGM

It remains to be explained why electrophysiological studies can detect CAD in the resting patient although the heart's flow reserve may prevent the coronary stenoses from being hemodynamically relevant at the time of examination. The pathophysiological mechanisms that theoretically lead to stunning, hibernating myocardium, and reversible mechanical dysfunction in patients with CAD have been discussed [12] and may provide a hypothetical explanation for the changes in CGM parameters recorded in the resting CAD patient.

Even in the absence of frank myocardial ischemia, atherosclerotic coronary lesions may induce electrophysiological changes in whole or as a correlate. For example, previous stress-induced ischemia may cause myocardial "stunning" effects. Coronary arteriosclerosis can be associated with myocardial small vessel disease that is not evident in the angiogram. Stenosis-induced changes in coronary and recipient myocardial perfusion may abnormally shift spatial potentials. Another, albeit speculative theory is that changes on the cellular level might affect the electrical membrane properties of myocytes in areas with mild chronic reduction of coronary flow.

In this study, we used coronary angiography—the gold standard for CAD diagnosis—to verify or exclude CAD in our patients because it best demonstrates the morphological coronary status. However, coronary angiography allows only limited conclusions to be drawn about the function and perfusion of the myocardium at rest and under stress. Some coronary stenoses may be of little significance for a stable blood and oxygen supply to the myocardium when collateral vessels have formed over the chronic course. On the other hand, the myocardium can be ischemic even though the coronary arteries are open, as e.g., in small vessel disease not evident in the angiogram.

Macrovascular coronary perfusion can only be estimated by the angiographic assessment of the vessel diameters and is only indirectly linked to electrical membrane phenomena. Therefore, further studies should not only measure CGM against angiography as a reference method, but also, against a method that functionally visualizes the perfusion of the myocardium (e.g., SPECT, stress MRI, or PET). We anticipate that CGM will correlate better with scintigraphic, than with coronary angiographic findings.

Our results proved that specific CGM parameters are significant and suitable for detecting predefined CAD categories and our systematically computed algorithm derived from a diagnostic set of stenosis pattern-specific, parallel and equally ranked parameters enables global CAD detection. Although not every parameter is useful for every category, the overall parameter set appears to be independent of coronary stenosis localization and distribution or ischemia pattern. Ongoing prospective studies evaluating cardiogoniometric detection of CAD in larger populations are focused on CAD pretest probabilities in primary care settings and different reference standards for visualising myocardial perfusion.

References

1. Austen WG, Edwards JE, Frye RL et al (1975) A reporting system on patients evaluated for coronary artery disease. Report of the Ad Hoc Committee for Grading of Coronary Artery Disease, Council on Cardiovascular Surgery, American Heart Association. Circulation 51:5–40
2. Chou TC, Helm RA, Kaplan S (1974) Clinical vectorcardiography, 2nd edn. Grune and Stratton, New York
3. Couderc JP, Zareba W, McNitt S et al (2007) Repolarization variability in the risk stratification of MADIT II patients. Europace 9(9):717–723
4. Davies SW (2001) Clinical presentation and diagnosis of coronary artery disease: stable angina. Br Med Bull 59:17–27
5. Drew BJ, Pelter MM, Lee E et al (2005) Designing prehospital ECG systems for acute coronary syndromes. Lessons learned from clinical trials involving 12-lead ST-segment monitoring. J Electrocardiol 38:180–185
6. Erikssen J, Müller C (1972) Comparison between scalar and corrected orthogonal electrocardiogram in diagnosis of acute myocardial infarcts. Br Heart J 34:81–86
7. Frank E (1956) An accurate, clinically practical system for spatial vectorcardiography. Circulation 13:737–749
8. Gibbons RJ, Balady GJ, Bricker JT et al (2002) ACC/AHA 2002 guideline update for exercise testing: summary article: a report of the American College of Cardiology/American Heart Association Task Force on Practice Guidelines (Committee to Update the 1997 Exercise Testing Guidelines). Circulation 106(14):1883–1892
9. Gray W, Corbin M, King J et al (1972) Diagnostic value of vectorcardiogram in strictly posterior infarction. Br Heart 34:1163–1169
10. Hinrikus H, Suhhova A, Bachmann M et al (2009) Electroencephalographic spectral asymmetry index for detection of depression. Med Biol Eng Comput 47(12):1291–1299
11. Howard PF, Benchimol A, Desser KB et al (1976) Correlation of electrocardiogram and vectorcardiogram with coronary occlusion and myocardial contraction abnormality. Am J Cardiol 38:582–587
12. Mazzadi AN, André-Fouët X, Costes N et al (2006) Mechanisms leading to reversible mechanical dysfunction in severe CAD: alternatives to myocardial stunning. Am J Physiol Heart Circ Physiol 291(6):H2570–H2582
13. McConahay DR, McCallister BD, Hallermann FJ et al (1970) Comparative quantitative analysis of the electrocardiogram and the vectorcardiogram. Correlations with the coronary arteriogram. Circulation 42:245–259

14. Mehta J, Hoffman I, Smedresman P et al (1976) Vectorcardiographic, electrocardiographic, and angiographic correlations in apparently isolated inferior wall myocardial infarction. Am Heart J 91:699–704
15. Murray RG, Lorimer AR, Dunn FG et al (1976) Comparison of 12-lead and computer-analysed 3 orthogonal lead electocardiogram in coronary artery disease. Br Heart J 38:773–778
16. Rissanen SM, Kankaanpää M, Meigal A et al (2008) Surface EMG and acceleration signals in Parkinson's disease: feature extraction and cluster analysis. Med Biol Eng Comput 46(9):849–858
17. Rubulis A. (2007) T-vector and T-loop morphology analysis of ventricular repolarization in ischemic heart disease. Sundbyberg, larseric Digital Print AB
18. Rubulis A, Jensen J, Lundahl G et al (2004) T vector and loop characteristics in coronary artery disease and during acute ischemia. Heart Rhythm 1(3):317–325
19. Sanz E, Steger JP, Thie W (1983) Cardiogoniometry. Clin Cardiol 6:199–206
20. Schüpbach WM, Emese B, Loretan P et al (2008) Non-invasive diagnosis of coronary artery disease using cardiogoniometry performed at rest. Swiss Med Wkly 138(15–16):230–238
21. Seeck A, Huebner T, Schuepbach M, et al. (2007) Nichtinvasive Diagnostik der koronaren Herzerkrankung mittels Kardiogoniometrie. In: Proceedings 41st DGBMT annual meeting. biomed tech. 5 2CD ROM: 47439
22. Seeck A, Garde A, Schuepbach M (2009) Diagnosis of ischemic heart disease with cardiogoniometry—linear discriminant analysis versus support vector machines. In: Vander Sloten J, Verdonck P, Marc Nyssen M, Haueisen J et al (eds) IFMBE proceedings. Springer, Berlin
23. Villella A, Maggioni AP, Villella M et al (1995) Prognostic significance of maximal exercise testing after myocardial infarction treated with thrombolytic agents: the GISSI-2 database. Gruppo Italiano per lo Studio della Sopravvivenza Nell'Infarto. Lancet 346:523–529
24. von Mengden HJ, Mayet W, Lippold K et al (1981) Pattern quantification of coronary artery stenosis by computerized analysis of multiple ECG parameters (author's transl). Klin Wochenschr 59:629–637
25. Wilson FN, Johnston FD (1938) The Vectorcardiogram. Am Heart J 16:14–28
26. World Health Organization. The 10 leading causes of death by broad income group (2004), Fact sheet N°310, Geneva, Updated October 2008
27. Zareba W, Badilini F, Moss AJ (1994) Automatic detection of spatial and dynamic heterogeneity of repolarization. J Electrocardiol 27(Suppl):66–72